Supplementary Information

Post-functionalization of organometallic complexes *via* click-reaction

Stanislav Petrovskii, Viktoria Khistiaeva, Aleksandra Paderina, Evgenia Abramova and Elena Grachova *

Institute of Chemistry, St Petersburg University, 198504 St. Petersburg, Russia

Correspondence: e.grachova@spbu.ru

Content

X-ray structure determination

The crystal structure of **Pt(dtpby)c** was determined by the means of single crystal X-ray diffraction analysis. Crystal was fixed on a micro mount and the diffraction data have been collected on the Agilent Supernova diffractometer at a temperature of 170K using monochromated Cu K_α radiation. Data were integrated and corrected for background, Lorentz, and polarization effects. An empirical absorption correction based on spherical harmonics implemented in the SCALE3 ABSPACK algorithm was applied in *CrysAlisPro* program [1]. The unit-cell parameters (Table S1) were refined by the least-squares techniques. The structure were solved by dual-space algorithm and refined using the *SHELX* programs [2,3] incorporated in the *OLEX2* program package [4].The final model included coordinates and anisotropic displacement parameters for all non-H atoms. The carbon-bound H atoms were placed in calculated positions and were included in the refinement in the 'riding' model approximation, U_{iso}(H) set to 1.5U_{eq}(C) and C–H 0.96 Å for the CH_3 groups, U_{iso}(H) set to 1.2U_{eq}(C) and C–H 0.97 Å for the CH_2 groups, U_{iso}(H) set to 1.2U_{eq}(C) and C–H 0.93 Å for the CH groups. Supplementary crystallographic data for this paper have been deposited at Cambridge Crystallographic Data Centre (CCDC 2204302) and can be obtained free of charge via www.ccdc.cam.ac.uk/structures/.

Table S1. Crystallographic data for compound **Pt(dtbpy)^{C}**.

Compound	**Pt(dtbpy)^{C}**
Formula	$C_{49}H_{52}N_{10}OPt$
Crystal system	monoclinic
a (Å)	11.56500(10)
b (Å)	20.6552(2)
c (Å)	18.3102(2)
α (°)	90
β (°)	99.1890(10)
γ (°)	90
V (Å^3)	4317.76(7)
Molecular weight	992.09
Space group (number)	$P2_1/n$ (14)
μ (mm^{-1})	6.473
Temperature (K)	170(100)
Z	4
ρ_{calc} (g/cm^{-3})	1.526
Crystal size (mm^3)	0.12×0.15×0.21
Diffractometer	SuperNova, Dual, Cu at zero, Atlas
Radiation	Cu K_α
Total reflections	71362
Unique reflections	8187
Angle range 2Θ (°)	6.50 to 140.00 (0.82 Å)
Reflections with $\|F_o\| \geq 4\sigma_F$	7906
R_{int}	0.0406
R_σ	0.0154
R_1 ($\|F_o\| \geq 4\sigma_F$)	0.0247
wR_2 ($\|F_o\| \geq 4\sigma_F$)	0.0645
R_1 (all data)	0.0254
wR_2 (all data)	0.0650
Goodness-of-fit on F^2	1.107
ρ_{max}, ρ_{min} (e/Å^3)	3.17/−0.62
CCDC number	2204302

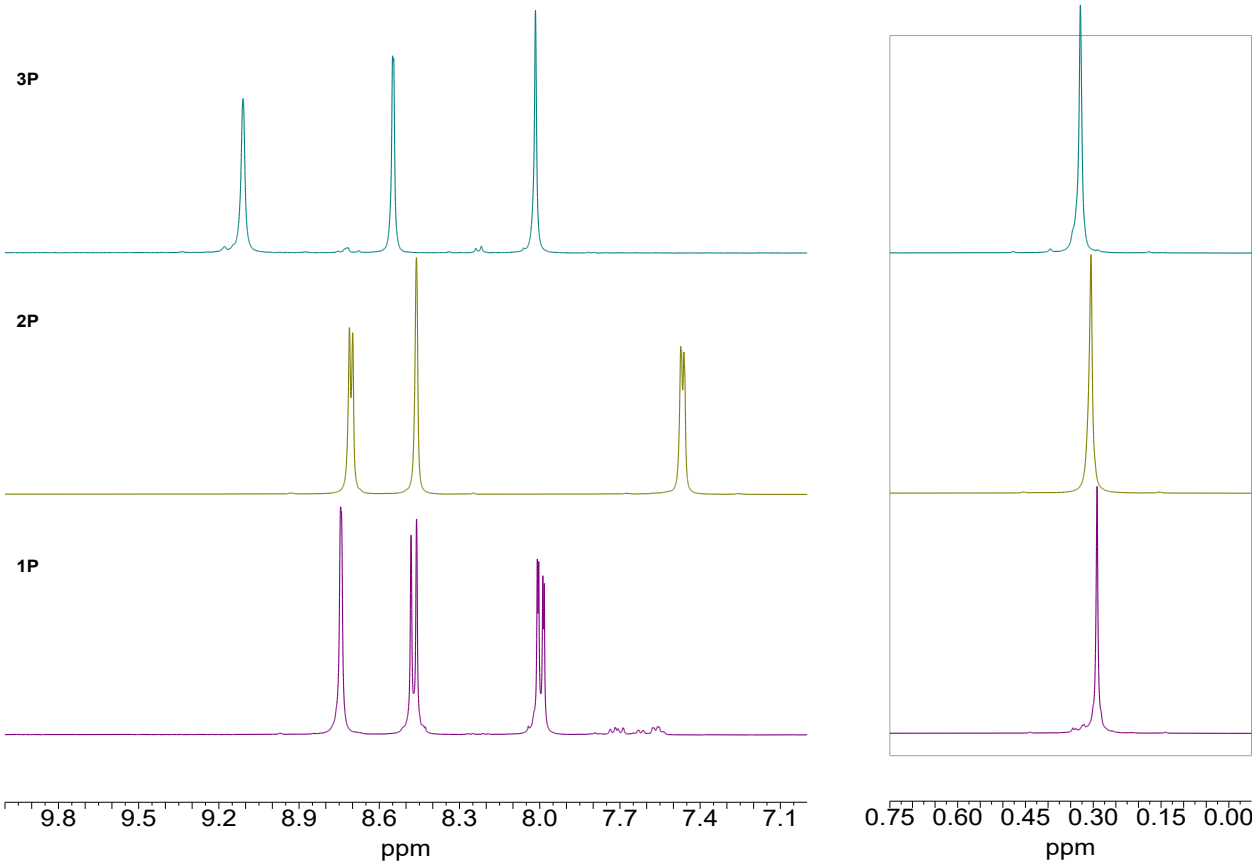

Figure S1. ^{1}H NMR spectra of **NN** compounds **XP** (X = 1−3). Aromatic (left) and aliphatic (right) regions are shown on a different vertical scale.

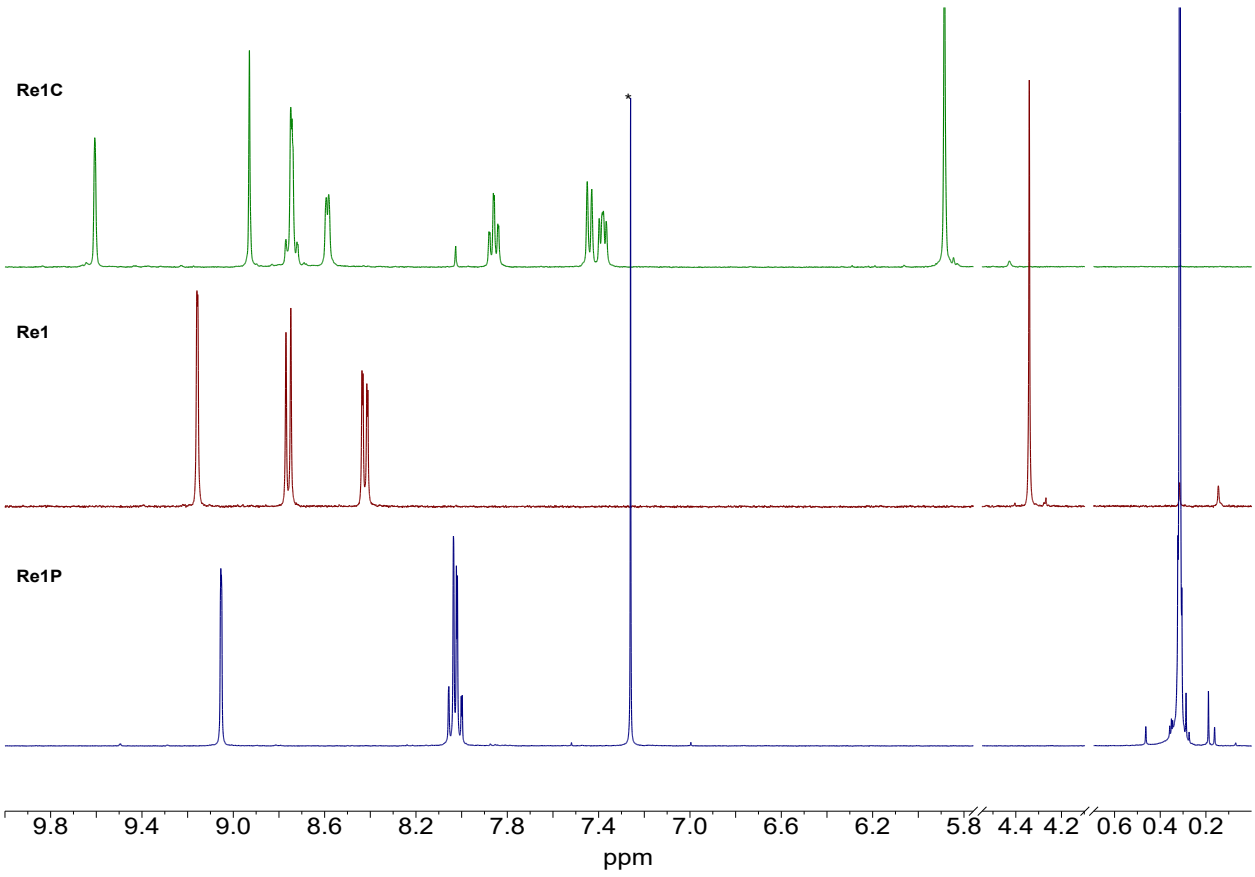

Figure S2. ^{1}H NMR spectra of **Re1^{X}** complexes. The residual solvent peak of $CDCl_3$ is marked by asterisk.

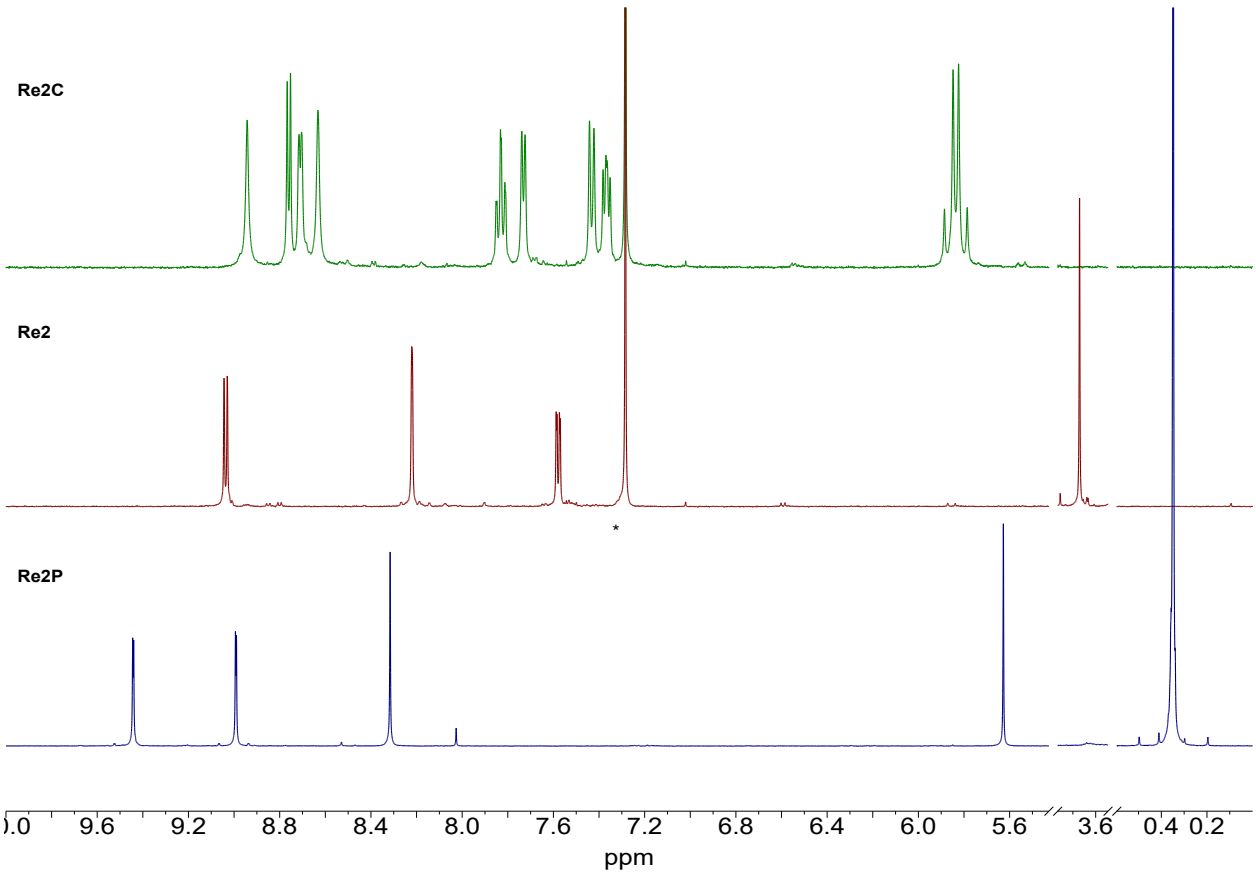

Figure S3. ^{1}H NMR spectra of **Re2^{X}** complexes. The residual solvent peak of $CDCl_3$ is marked by asterisk.

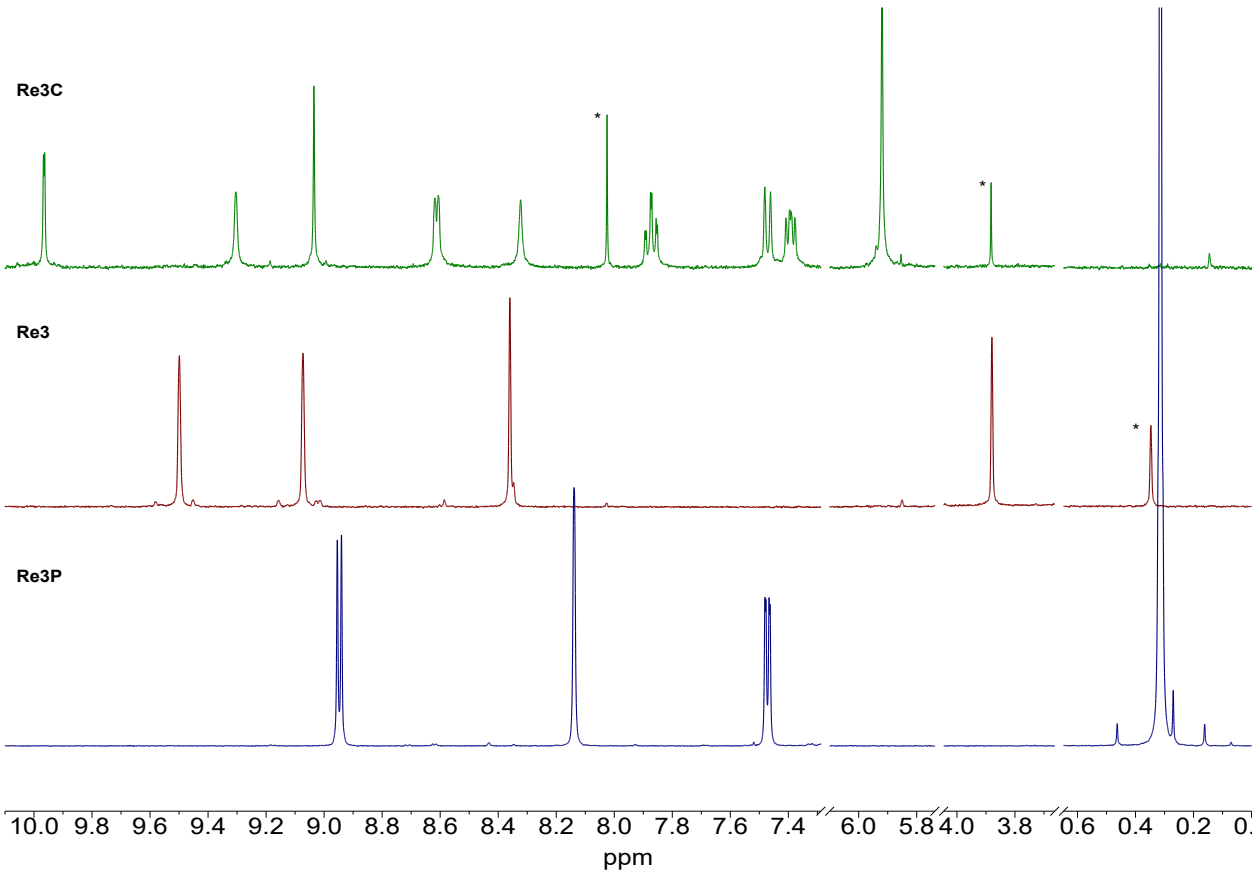

Figure S4. ^{1}H NMR spectra of **Re3^{X}** complexes. The resonances of admixtures are marked by asterisks.

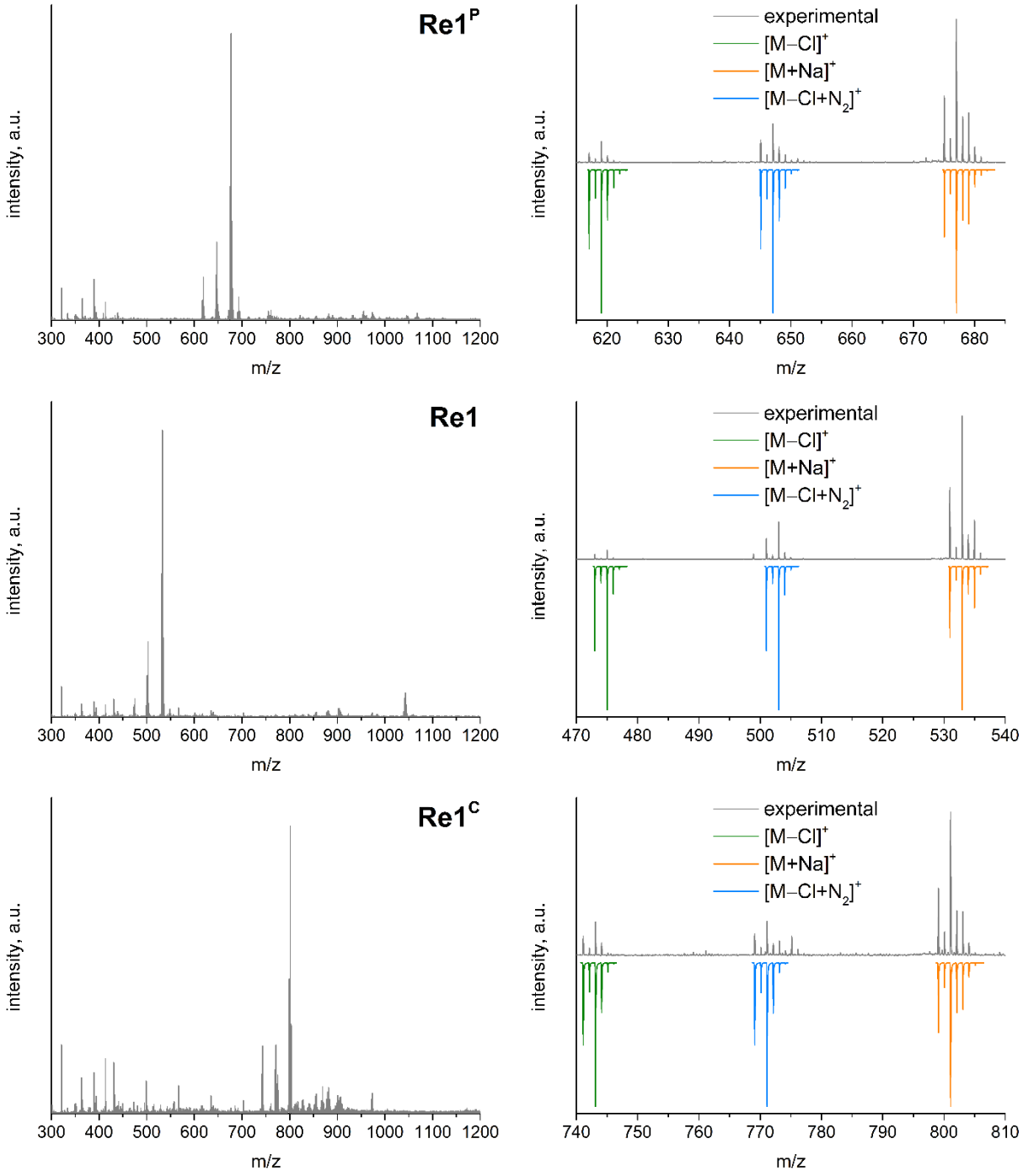

Figure S5. ESI$^+$ MS spectra of **Re1^X** complexes with isotope pattern of key signals.

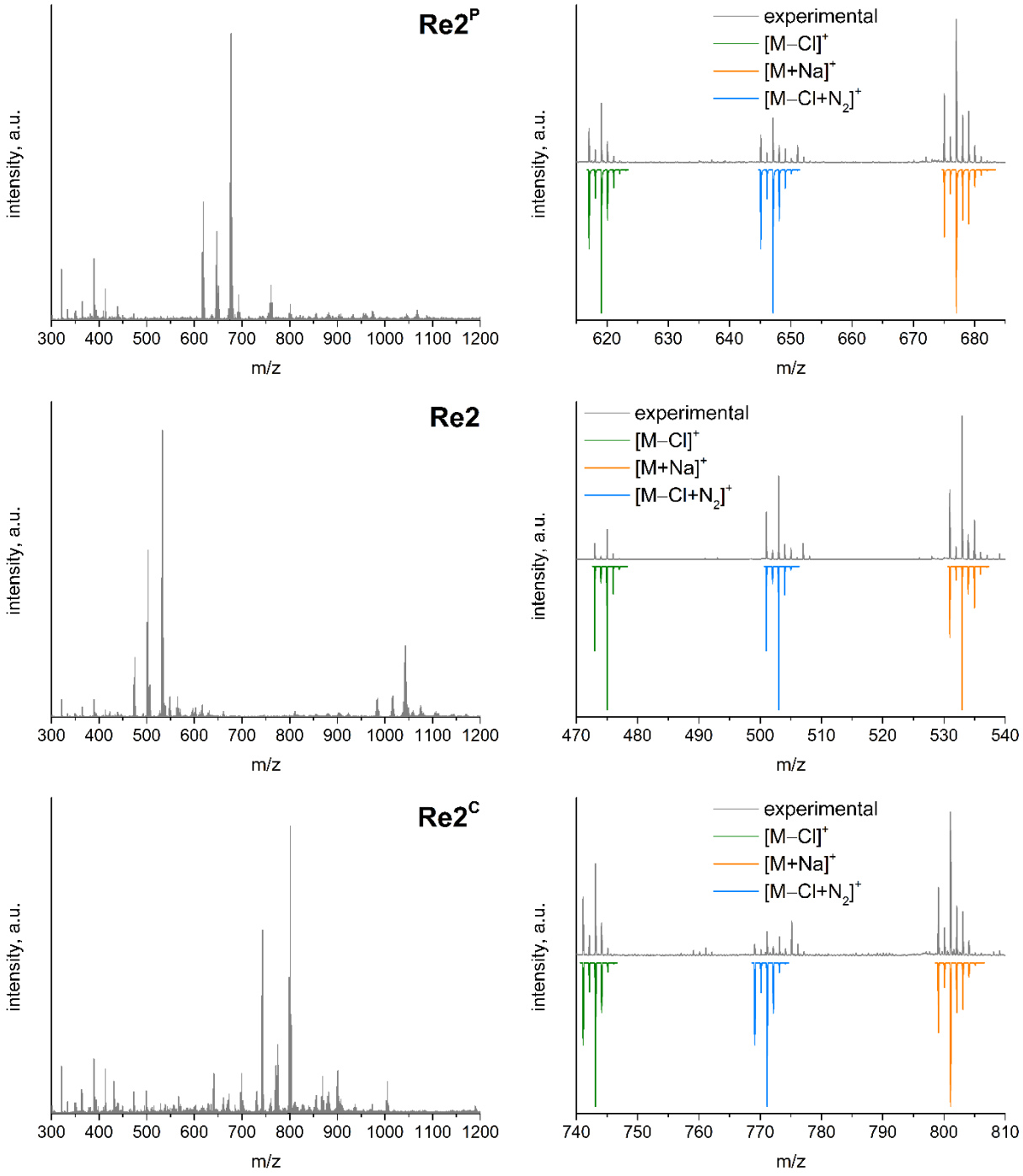

Figure S6. ESI$^+$ MS spectra of **Re2^X** complexes with isotope pattern of key signals.

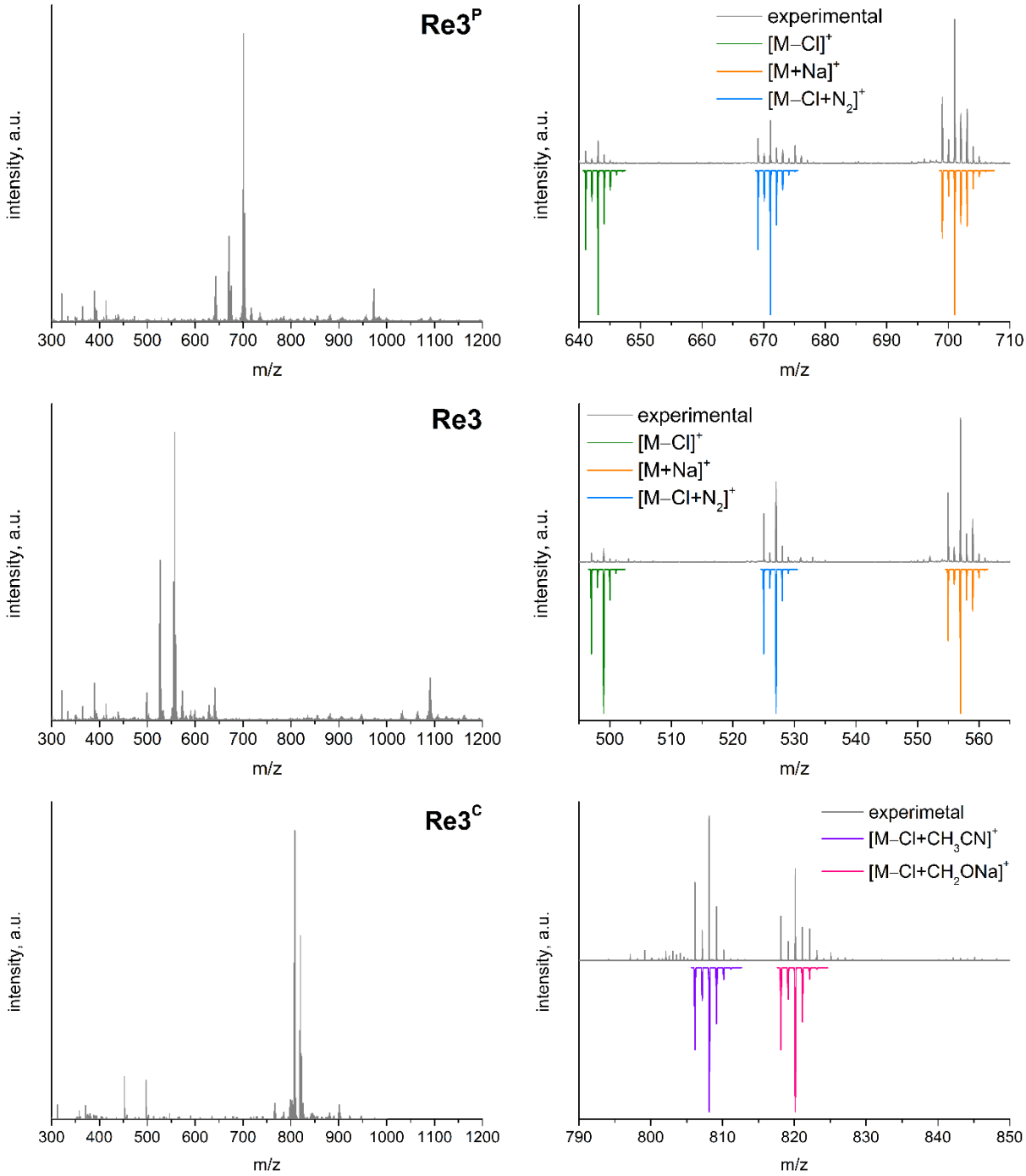

Figure S7. ESI$^+$ MS spectra of **Re3^X** complexes with isotope pattern of key signals.

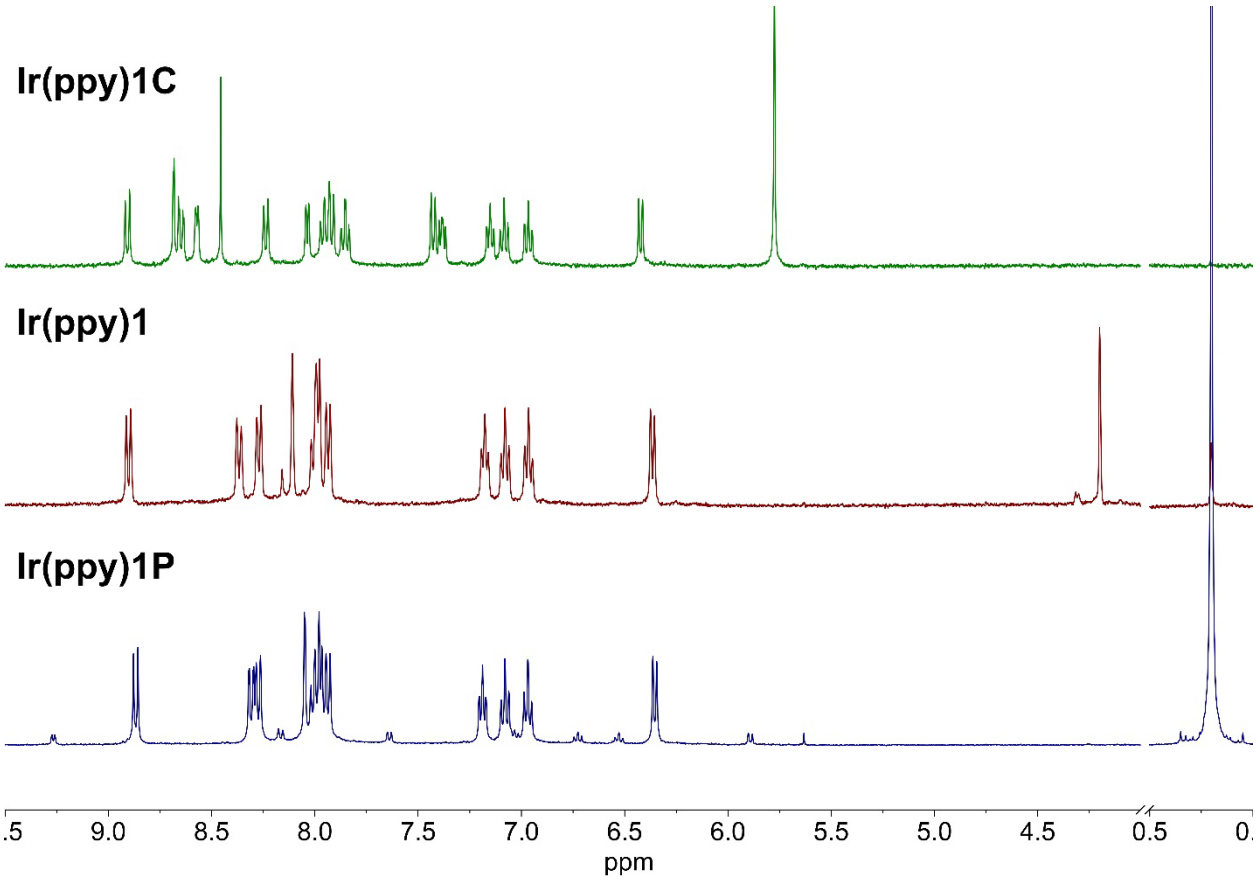

Figure S8. ^{1}H NMR spectra of **Ir(ppy)1^{X}** complexes.

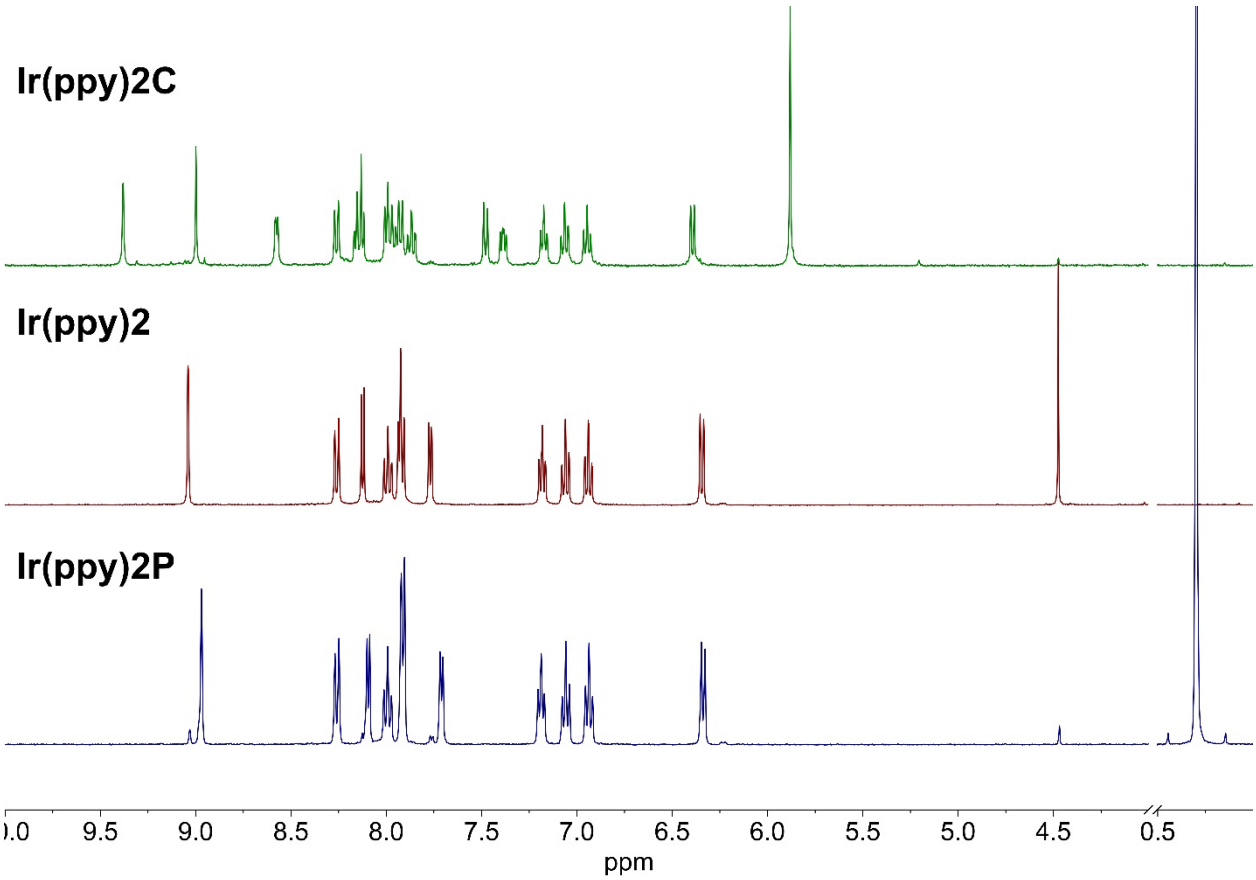

Figure S9. ^{1}H NMR spectra of **Ir(ppy)2^{X}** complexes.

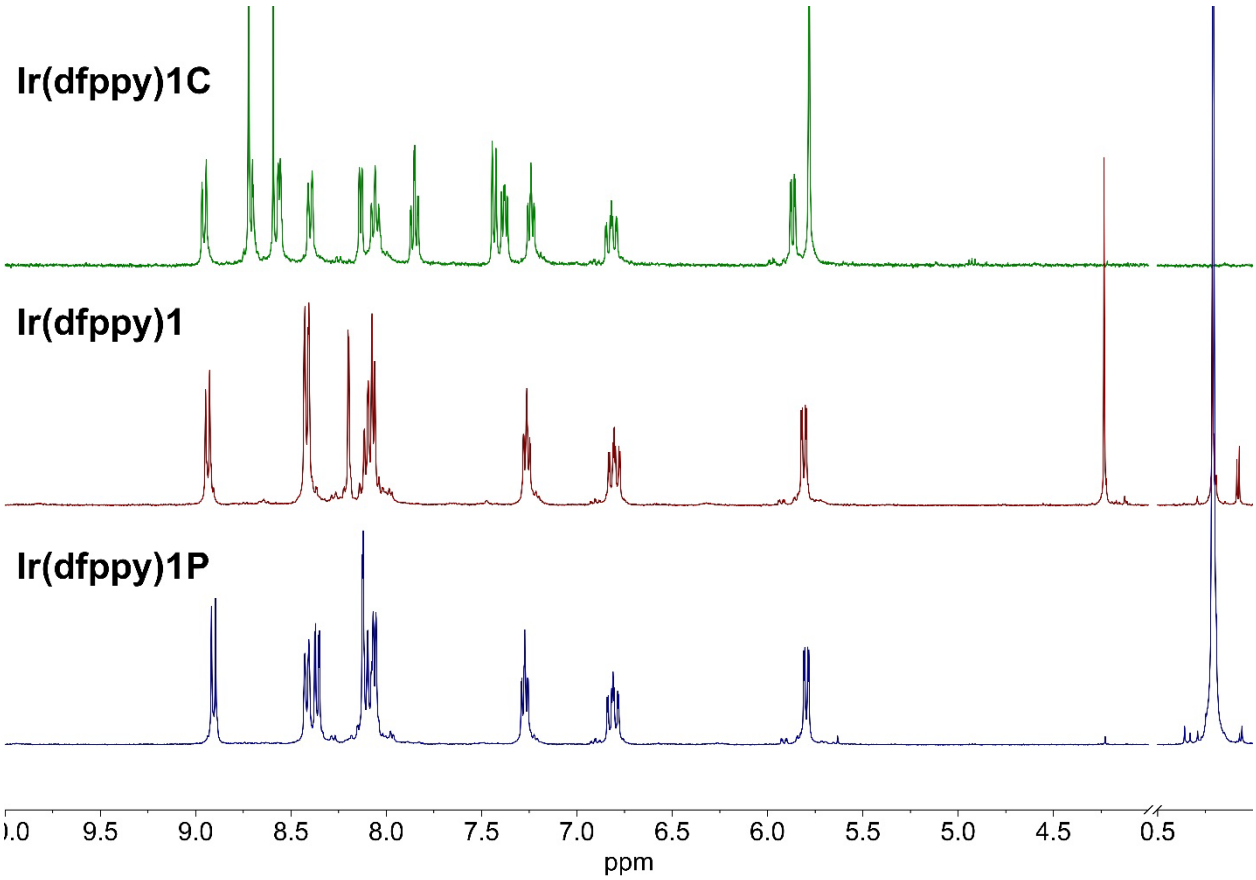

Figure S10. ^{1}H NMR spectra of **Ir(dfppy)1^{X}** complexes.

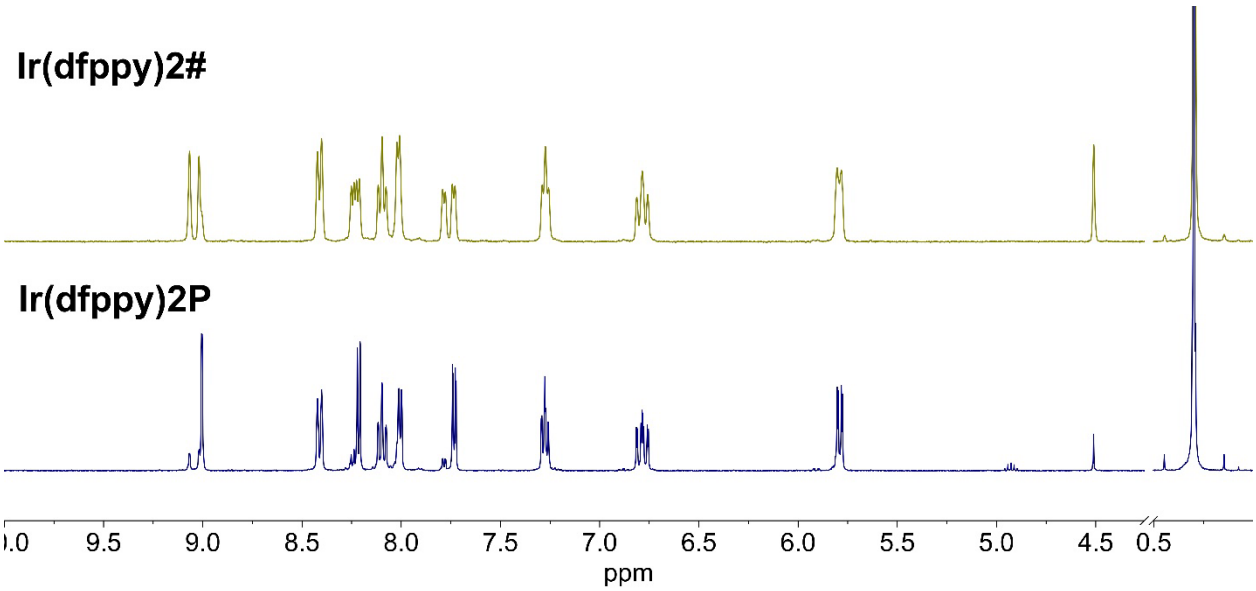

Figure S11. ^{1}H NMR spectra of **Ir(dfppy)2^{X}** complexes.

$^{\#}$Mixture of **Ir(dfppy)2^{P}** and **Ir(dfppy)2**.

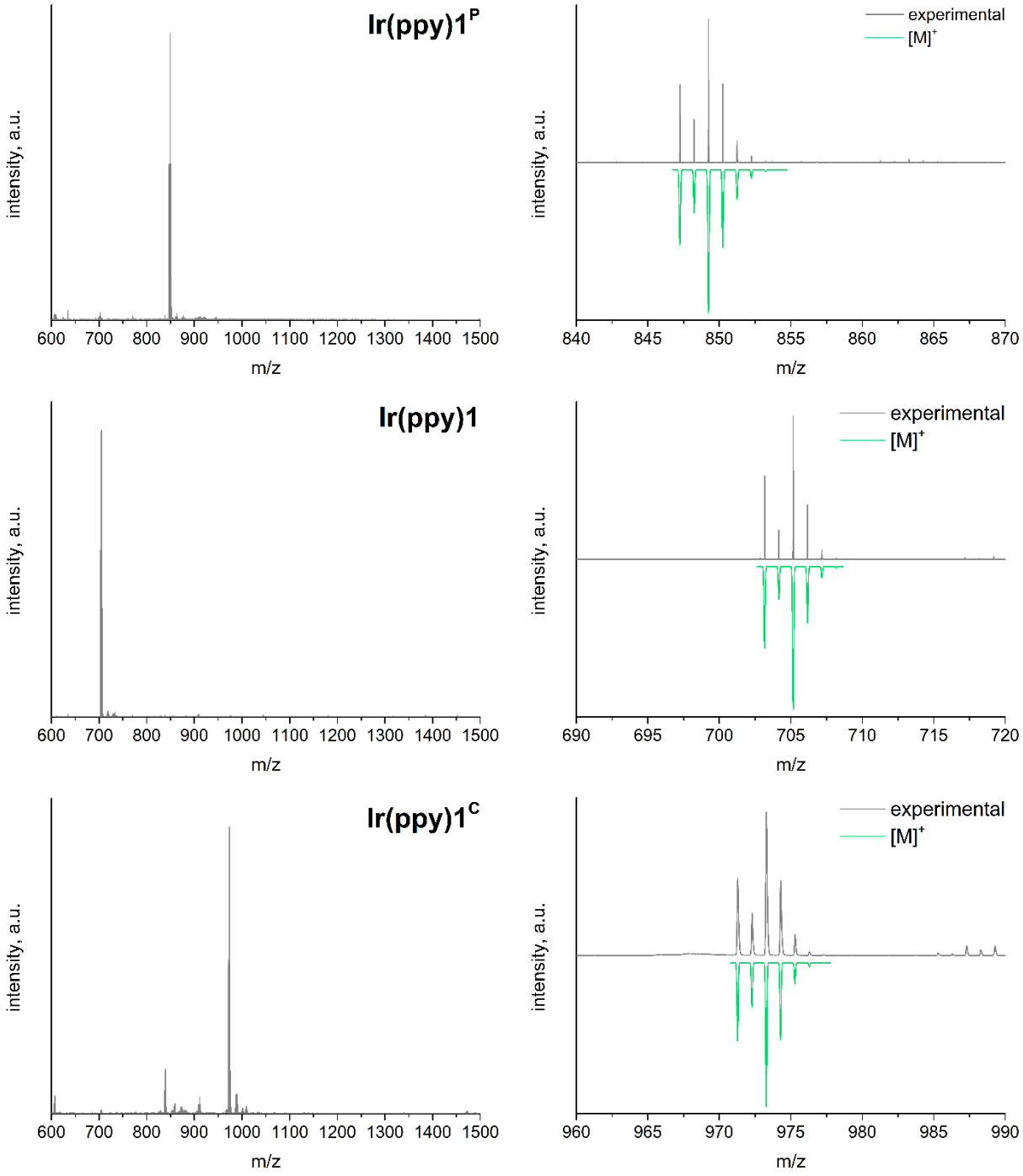

Figure S12. ESI$^+$ MS spectra of **Ir(ppy)1^X** complexes with isotope pattern of key signals.

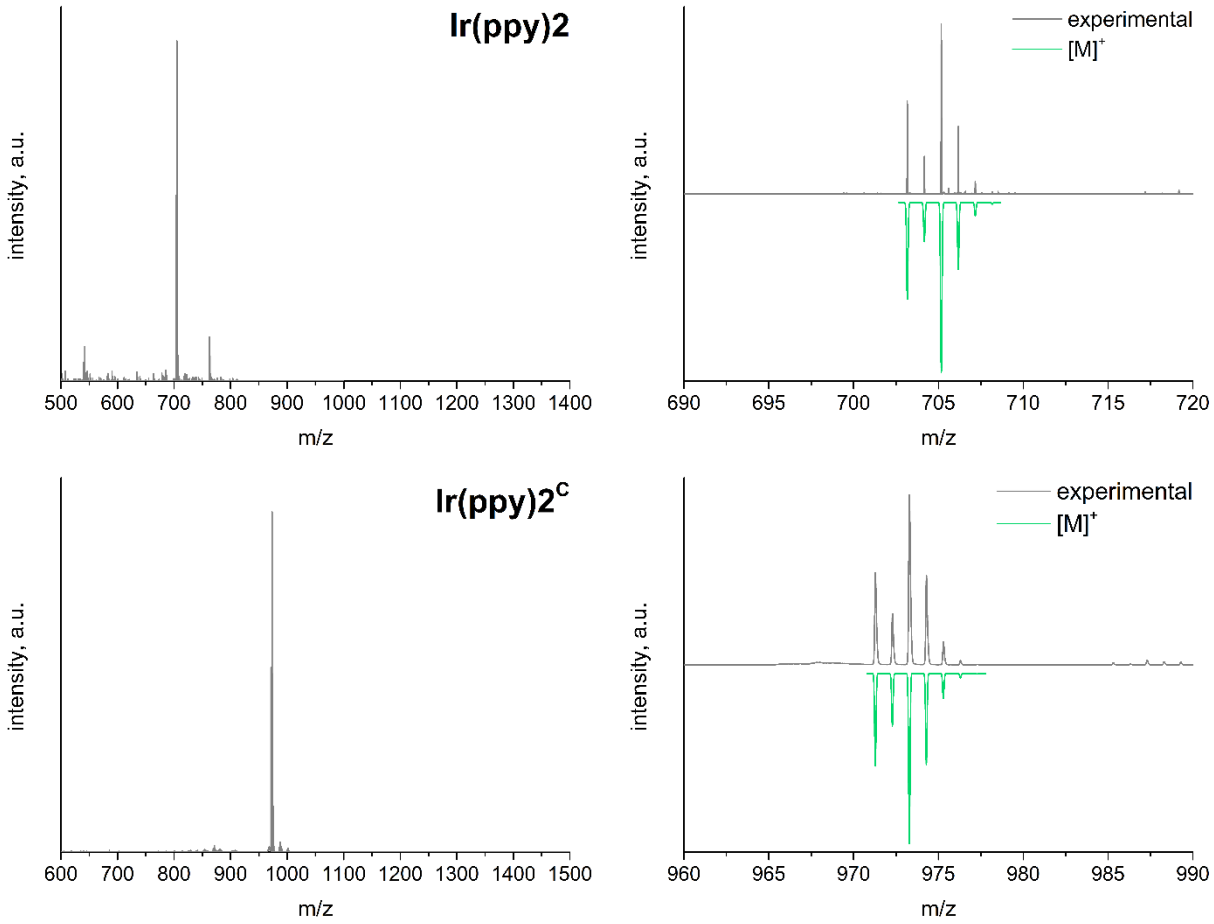

Figure S13. ESI$^+$ MS spectra of **Ir(ppy)2^X** complexes with isotope pattern of key signals.

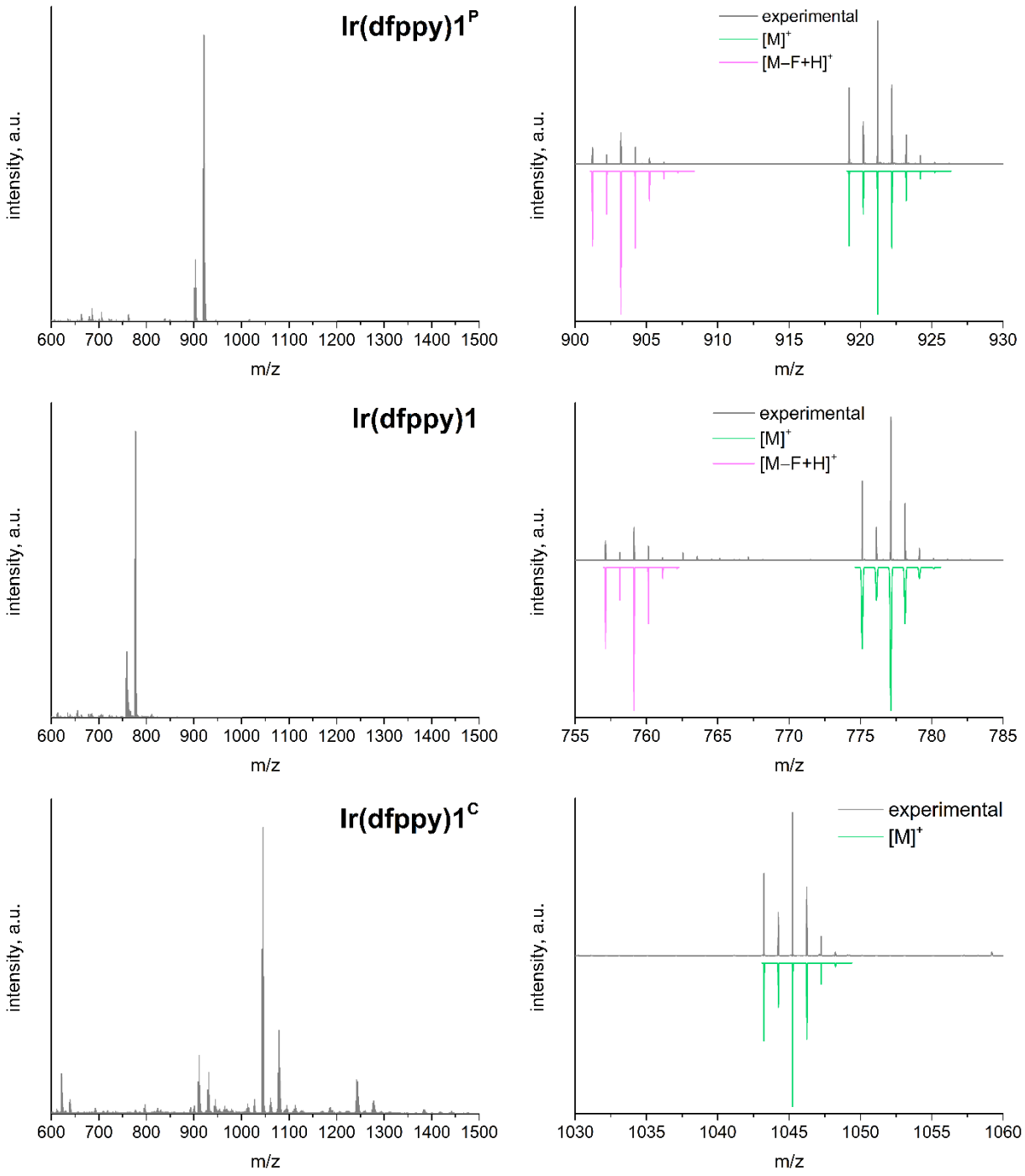

Figure S14. ESI$^+$ MS spectra of **Ir(dfppy)1^X** complexes with isotope pattern of key signals.

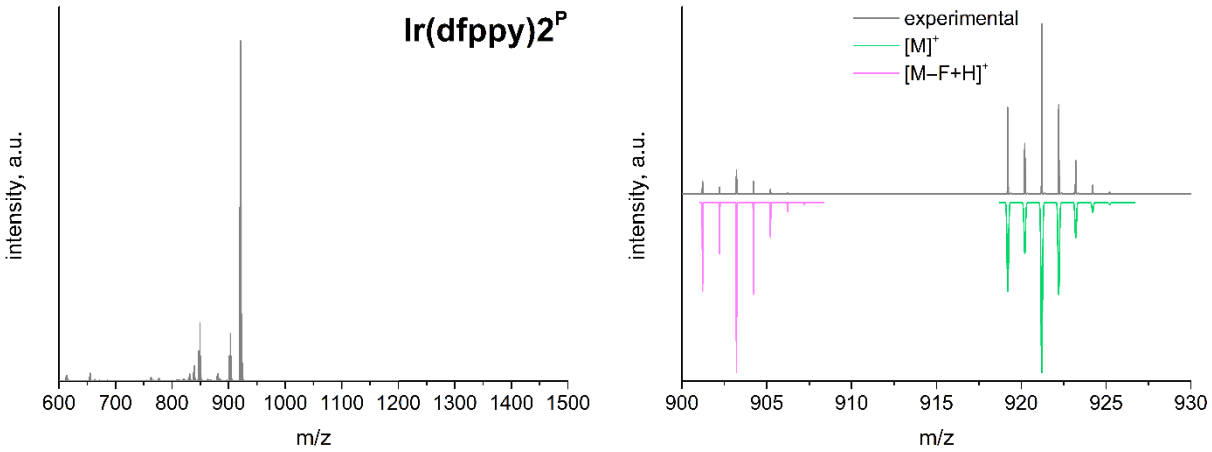

Figure S15. ESI$^+$ MS spectra of **Ir(dfppy)2^P** complexes with isotope pattern of key signals.

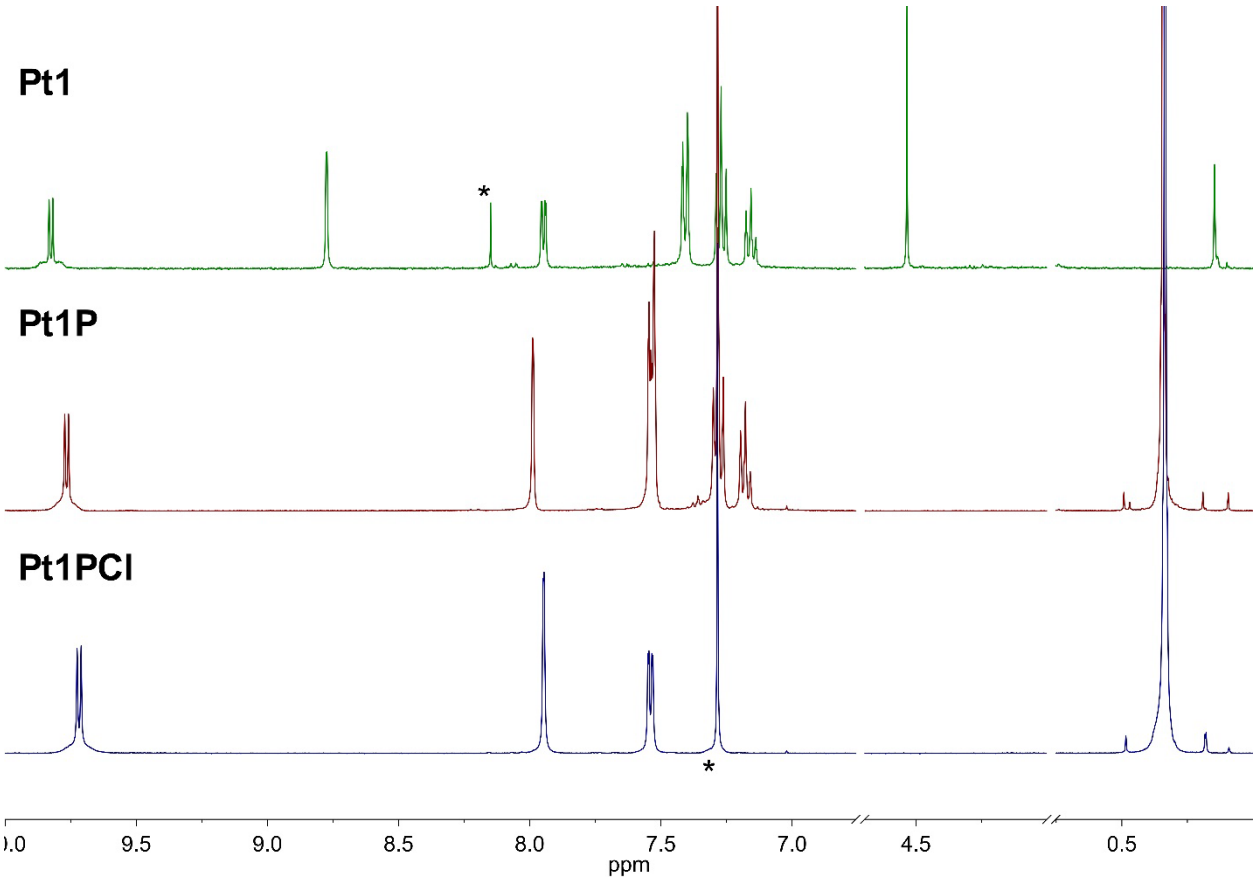

Figure S16. ^{1}H NMR spectra of **Pt1^{X}** complexes. Asterisks mark the resonances of admixtures and the residual solvent peak of $CDCl_3$ (7.29 ppm).

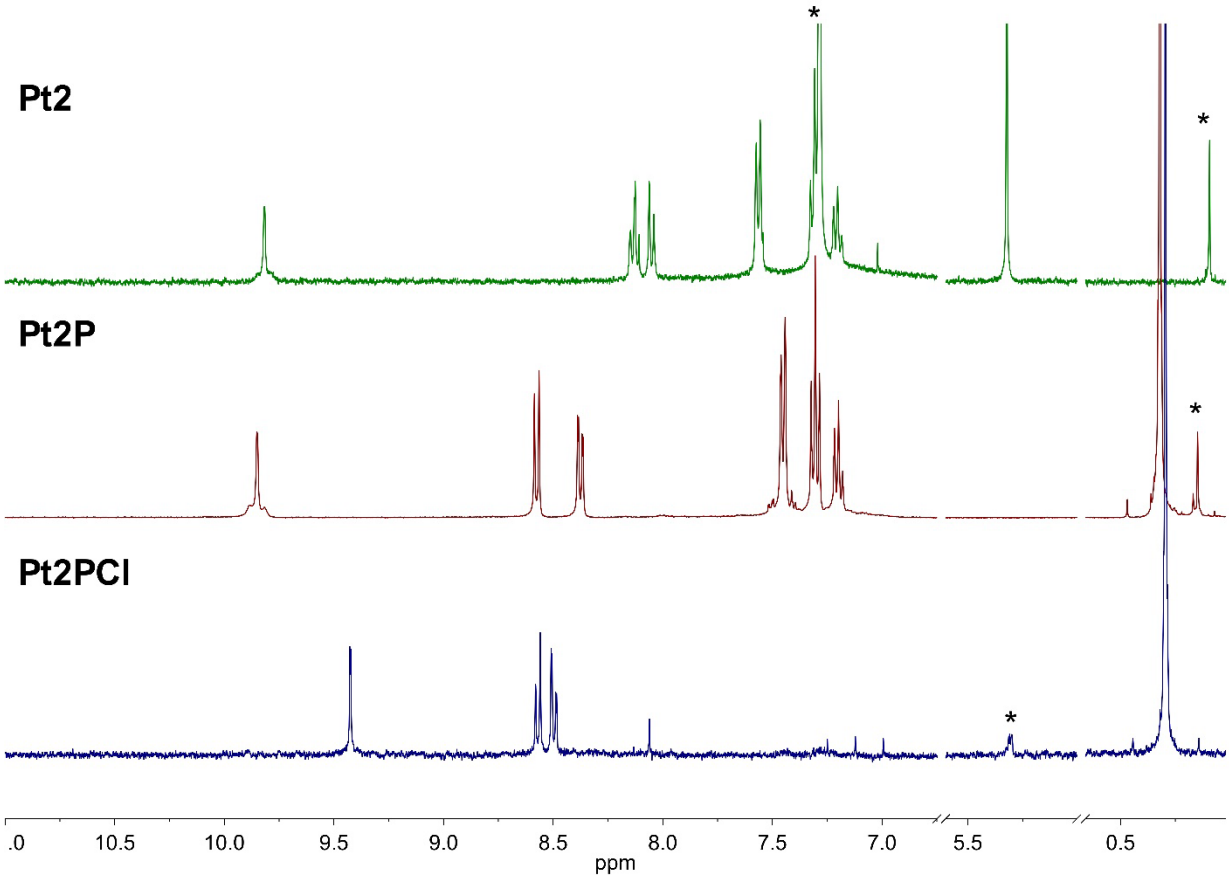

Figure S17. ^{1}H NMR spectra of **Pt2^{X}** complexes. Asterisks mark the resonances of admixtures and the residual solvent peak of $CDCl_3$ (7.29 ppm).

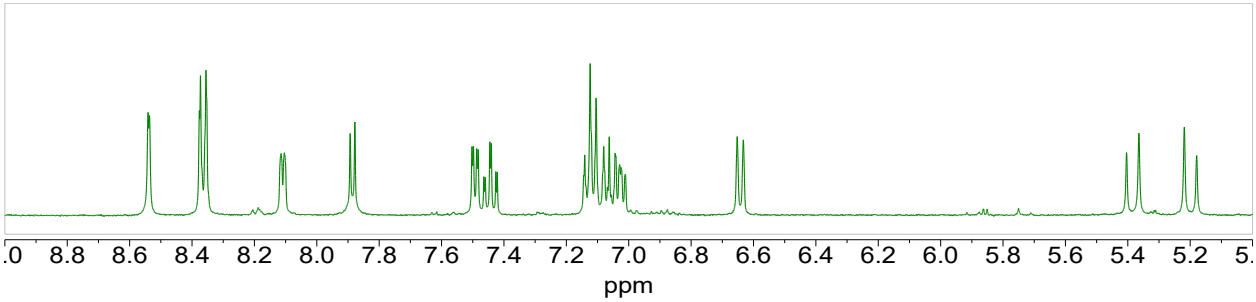

Figure S18. ^{1}H NMR spectrum of **Pt(btbpy)^{C}** complexes in aromatic region, DMSO-d_6, RT.

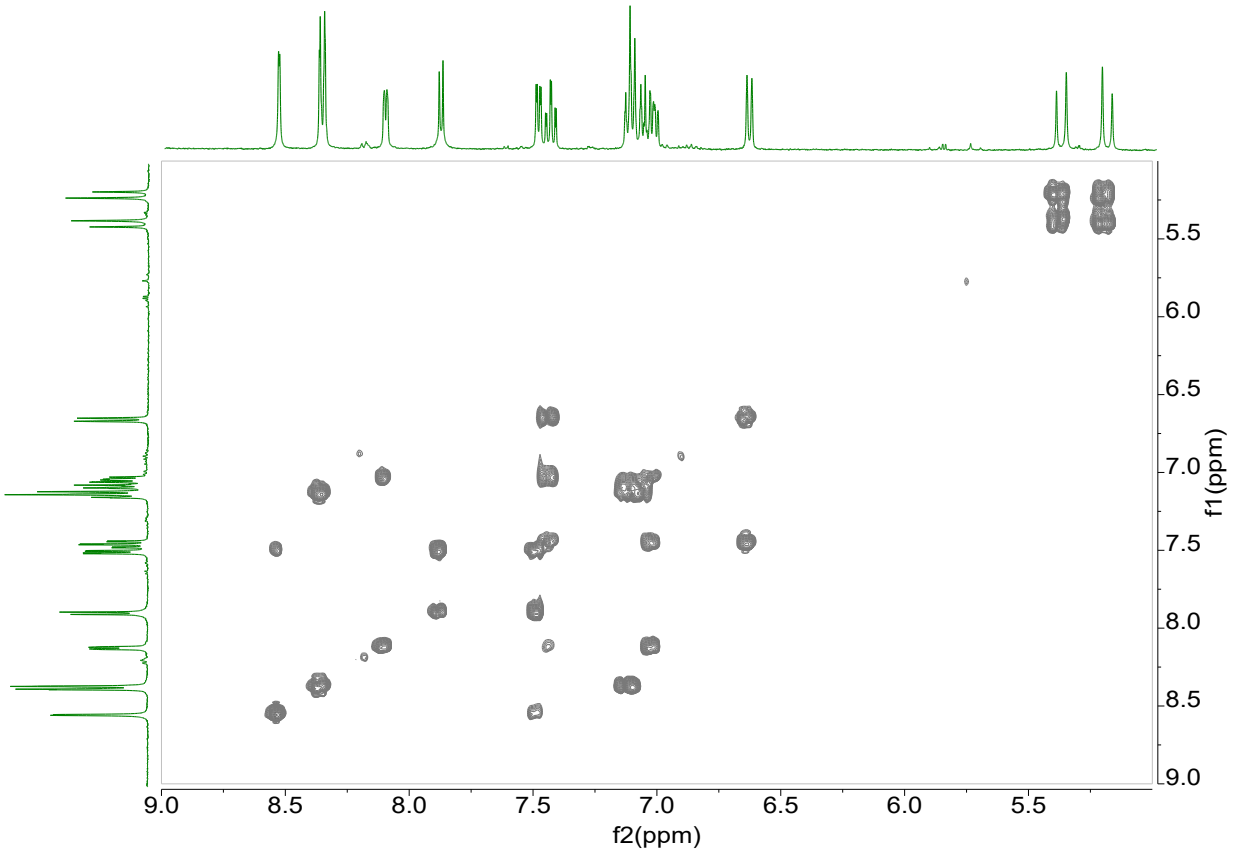

Figure S19. ^{1}H^{1}H COSY NMR spectrum of **Pt(btbpy)^{C}** complexes in aromatic region, DMSO-d_6, RT.

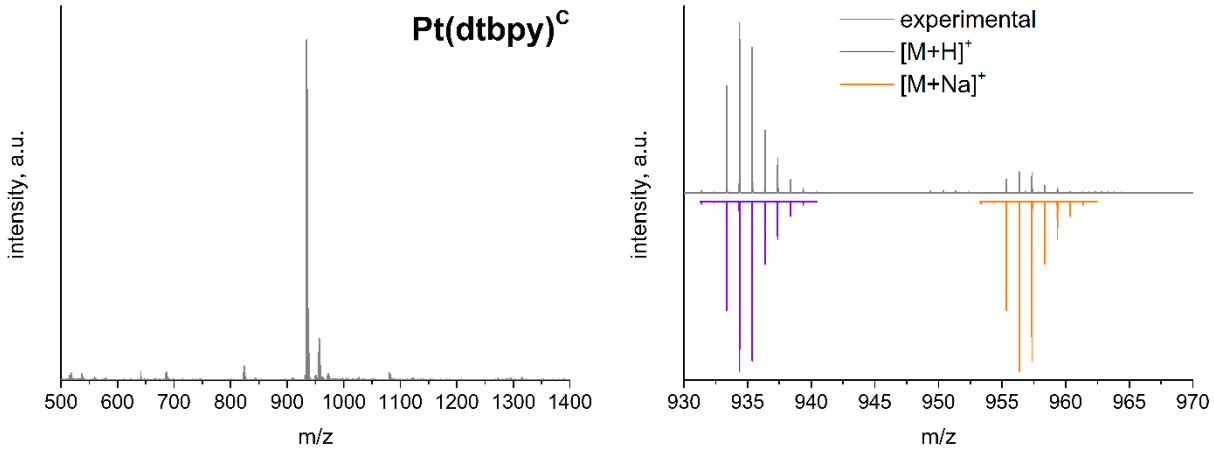

Figure S20. ESI$^+$ MS spectrum of **Pt(dtbpy)^C** complex with isotope pattern of key signals.

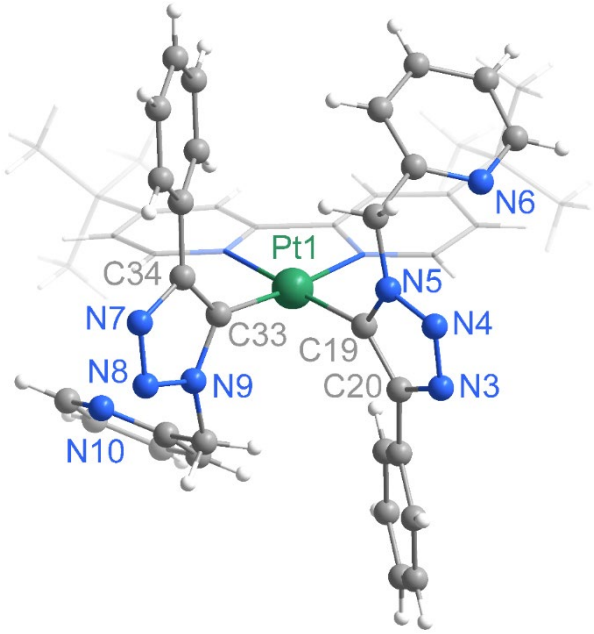

Figure S21. Molecular structure of **Pt(dtbpy)^C** complex with key atoms numeration.

Table S2. Selected structural parameters for compound **Pt(dtbpy)^{C}** and literature data for Pt(II) triazolyl derivatives [5,6].

Bond lengths, Å		**Literature reported range, Å**
Pt1–N1	2.078(2)	1.959 – 2.077
Pt1–N2	2.079(2)	
Pt1–C19	2.010(2)	1.989 – 2.007
Pt1–C33	2.001(3)	
C19–C20	1.394(4)	1.376 – 1.407
C33–C34	1.394(4)	
N3–N4	1.305(3)	1.306 – 1.322
N7–N8	1.309(3)	
N4–N5	1.354(3)	1.351 – 1.386
N8–N9	1.354(3)	
Bond angles, °		**Literature data, °**
N1–Pt1–N2	78.29 (9)	76.86
C19–Pt1–C40	88.02(10)	88.55
Plane angle, °		**Literature data, °**
Pt-N1-N2 ring–C19 ring	95.543	87.38
Pt-N1-N2 ring–C33 ring	95.586	

Table S3. Photophysical properties of "clicked" complexes **ReX^{C}** and **IrX^{C}**, DCE, r.t., 10^{-5} M.

	λ, nm (ε, 10^{-3} cm^{-1}M^{-1})	**λ_{em}, nm**	**Φ, %**		**τ, μs**	
			A	**D**	**A**	**D**
Re1^{C}	291 (28.5), 351 (31.8), 365 (32)	660	<1	<1	0.24	0.22
Re2^{C}	291 (43.4)	650	<1	<1	0.49	0.52
Re3^{C}	280 (47.8), 342 (31.8)	645	<1	<1	0.88	0.87
Ir(dfppy)1^{C}	252 (33.9), 307 (25.3), 357 (26.1)	533	7.7	42.7	0.79	2.14
Ir(ppy)1^{C}	254 (65.7), 297 (50.8), 343 (42.5), 357 (43.1)	626	7.7	19.2	0.22	0.35
Ir(ppy)2^{C}	267 (94.4), 365 (18.8)	609	7.1	37.9	0.22	0.42

A = aerated. D = degassed.

References

1. *CrysAlisPro, Rigaku Oxford Diffraction*; Agilent Technologies: Version 1.171.39.35a, 2017;
2. Sheldrick, G.M. SHELXT - Integrated space-group and crystal-structure determination. *Acta Crystallogr. Sect. A Found. Crystallogr.* **2015**, *71*, 3–8, doi:10.1107/S2053273314026370.
3. Sheldrick, G.M. Crystal structure refinement with SHELXL. *Acta Crystallogr. Sect. C* **2015**, *71*, 3–8, doi:10.1107/S2053229614024218.
4. Dolomanov, O. V.; Bourhis, L.J.; Gildea, R.J.; Howard, J.A.K.; Puschmann, H. OLEX2 : a complete structure solution, refinement and analysis program. *J. Appl. Crystallogr.* **2009**, *42*, 339–341, doi:10.1107/S0021889808042726.
5. Li, Y.; Tsang, D.P.; Chan, C.K.; Wong, K.M.; Chan, M.; Yam, V.W. Synthesis of Unsymmetric Bipyridine–Pt II –Alkynyl Complexes through Post-Click Reaction with Emission Enhancement Characteristics and Their Applications as Phosphorescent Organic Light-Emitting Diodes. *Chem. – A Eur. J.* **2014**, *20*, 13710–13715, doi:10.1002/chem.201404315.
6. Guha, R.; Defayay, D.; Hepp, A.; Müller, J. Targeting Guanine Quadruplexes with Luminescent Platinum(II) Complexes Bearing a Pendant Nucleobase. *Chempluschem* **2021**, *86*, 662–673, doi:10.1002/cplu.202100135.